The IRM Quarterly

Spring 1999, Vol. 9, No. 1 Institute for Rock Magnetism
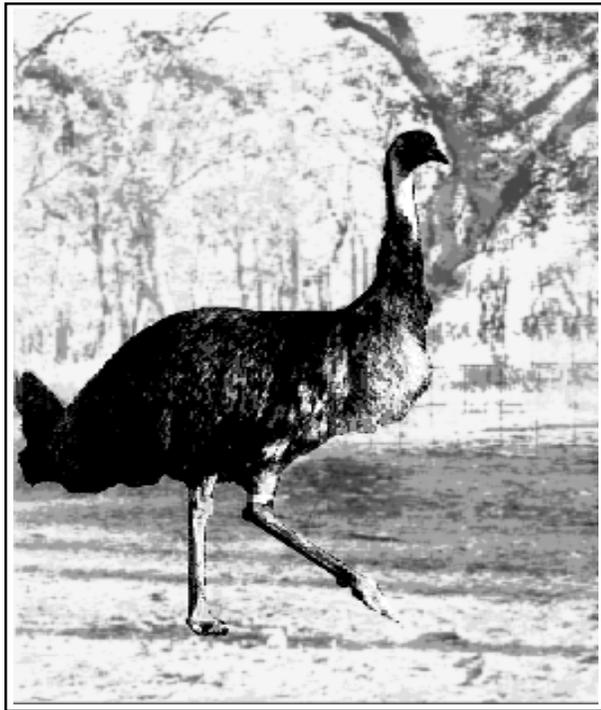
Dromiceius novaehollandae, *an Australian ratite (large flightless bird), resembling and related to the ostrich. Commonly known as the* **emu**.

Measure for Measure:

The Beauty of Magnetic Units

Mike Jackson
IRM

"*...when you can measure what you are speaking about and express it in numbers you know something about it; but when you cannot... your knowledge is of a meagre and unsatisfactory kind.*" - Kelvin

E.A. Burtt [1924] asserted that "the most stupendous single achievement of the human mind" was Newton's development of the mathematical laws of motion. From the great diversity of phenomena including planetary orbits, oscillating pendulums and falling apples, Newton distilled succinct mathematical relations to describe *all* motion, reduced to the fundamental quantities of length, mass, and time. These quantities represent the basic physical *dimensions* of mechanics, and from these are built concepts such as force, momentum and energy. It is the dimensionality of a physical variable that captures its essence, and the particular choice of units affects only its numerical value.

Force, for example, is quantified by the product of the acceleration it produces in a body and the body's mass; thus, whether given in units of pounds, dynes, or Newtons, force always has dimensions of LMT^{-2} (length*mass/time^2).

Roughly 150 years after Newton's *tour de force*, Gauss performed a similarly remarkable feat by showing that the Earth's magnetic field (and magnetic quantities in general) could be measured absolutely, in terms of *the same* fundamendal dimensions of length, mass and time. After Halley's mapping of magnetic declination ca 1700, shipborne magnetic field measurements became common, and by the late 18th century, measurements were being made of relative intensity of the field over the Earth's surface. These relative intensity measurements were based on the period of oscillation of a suspended magnetic needle, in much the same way that gravity measurements are made using a pendulum: the stronger the field, the more rapid the oscillations. Alexander von Humboldt made such magnetic measurements on his expeditions in South America and Asia, and proposed a relative unit of intensity, defined by reference to a standard value at Micuipampa, Peru (which, being situated nearly on the magnetic equator, had the lowest relative intensity measured by Humboldt; in these normalized units, global surface intensities ranged upward from unity).

We no longer measure magnetic field strength in Micuipampa units, primarily due to the work of Gauss. In 1829, Gauss began a fourteen-year period of intensive work on geomagnetism. In addition to the establishment of absolute measurements, his chief contributions (summarized by Garland [1979]) include spherical harmonic analysis of the geomagnetic field (enabling quantification of internal and external field sources, as well as dipole and non-dipole field components) and the organization of magnetic observatories to monitor changes in the field with time. His collaboration with Weber began in 1831, and in the following year Gauss

presented his classic "*Intensitas vis magneticae terrestris ad mensuram absolutam revocata*" before the Royal Society of Göttingen.

Absolute Magnetic Field Measurements

The period of oscillation of a compass needle with magnetic moment m and inertial moment I, in a magnetic field B, is:

$$T = 2\pi(I/mB)^{1/2}$$

This enables the product mB to be determined from measurement of T and I. *Relative* measurement of the field B is possible when m is unknown but assumed constant. To obtain an *absolute* measure of B, separate determination of m is required, and Gauss accomplished this through the use of a second magnetic compass. The first compass needle, whose moment is to be determined, is held with a fixed orientation at a distance d from the second compass, whose needle is thereby deflected. The deflection angle θ is independent of the magnetic moment of the second compass needle, depending only on the ratio m/B and the experimental geometry. Combining the two experiments enables separate determination of m and B, the latter being:

$$B = ((8\pi^2 I)/(d^3 \sin\theta T^2))^{1/2}$$

from which the dimensions of magnetic field follow: $L^{-1/2}M^{1/2}T^{-1}$. Gauss worked with units of milligrams, millimeters, and seconds, so his unit of B (mm$^{-1/2}$mg$^{1/2}$s^{-1}) corresponded to one tenth of the "cgs" unit now known as the Gauss (cm$^{-1/2}$g$^{1/2}$s^{-1}). The derived unit for magnetic moment m in the cgs system is called the emu (electro-magnetic unit); 1 emu = 1 cm$^{5/2}$g$^{1/2}$s^{-1}.

If you consult Garland's article for more details, you will observe that the field is there referred to as H (magnetic field), which I have here carefully changed to B (properly, magnetic induction, or flux density). Why?

Units

Visiting Fellows' Reports

Alexei Smirnov
University of Rochester
alexei@earth.rochester.edu

LOW-TEMPERATURE MAGNETIC PROPERTIES OF PELAGIC SEDIMENTS (ODP SITE 805C)

One mechanism which may bias sedimentary paleomagnetic records is the precipitation of single-domain (SD) magnetite produced by magnetotactic bacteria. This magnetite may carry a strong magnetization that is younger than the paleomagnetic signal formed in the post-depositional lock-in zone. To investigate this phenomenon we are studying carbonate oozes from the western equatorial Pacific Ocean. Transmission electron microscope (TEM) observations have demonstrated the presence of biogenic magnetite (magnetosomes) throughout the sediment column. They are especially abundant near the iron redox boundary (Tarduno and Wilkison, 1996; Tarduno et al., 1998). However TEM analyses are time consuming and do not yield unambiguous results for some particles. So the primary goal of our visit to the IRM was to investigate the distribution and amount of bacterial magnetite using low-temperature techniques (Moskowitz et al., 1993).

Low-temperature magnetic properties were measured on a MPMS-2. Saturation isothermal remanent magnetization (SIRM) was given to the samples in a strong magnetic field (2.5T) at 20K after cooling both in the absence (zero field cooling, ZFC) and presence of a 2.5T magnetic field (field cooling, FC). The thermal demagnetization of both ZFC and FC SIRM (further, ZFC and FC curves) was measured from 20K to 300K in a zero field environment.

A significant divergence between ZFC and FC curves was observed for all samples (Figure 1). For most samples the divergence disappears at room temperature. The area between the ZFC and FC curves, both normalized to the FC SIRM imparted at 20 K, was calculated and plotted versus depth. No statistically significant change was observed suggesting that the degree of the divergence does not depend on depth. The changes occurring during sample cooling in a strong magnetic field are reversible. The ZFC SIRM thermal demagnetization curves, measured before and after the thermal demagnetization of FC SIRM, coincide. Thus, the cooling of the sediment in a strong (saturating) magnetic field results in a reversible change of the magnetic state of the magnetic carrier. We believe that this phenomena is related to the stabilization of spontaneous magnetization vectors (M_s) with cooling. The application of a strong magnetic field to pseudo-single-domain grains at room temperature converts them to a meta-stable single-domain state. With cooling, the stabilization of spontaneous magnetization vectors (M_s) (i.e. adaptation of the defect structure to the spin configuration) occurs. The stabilization increases the M_{rs}/M_s ratio. Consequently, the value of FC SIRM imparted at low temperature after field cooling should be higher than ZFC SIRM. As a sediment warms in a zero field, the reverse process occurs and particles are gradually returned to their initial PSD state. The fact that the ZFC and FC curves converge only at room temperature (more exactly at the temperature when the field was turned on during the field cooling) suggests a constant distribution of stabilization temperatures over the entire temperature range.

In oxidized, non-stoichiometric magnetite the number of defects is greater than in stoichiometric magnetite (especially in the case of diffuse maghemitization), so the latter would have lower M_{rs}/M_s ratio in comparison with maghemitized magnetite. However, it is not clear if the presence of more defects can alone result in the observed divergences. The fact that maghemite does not manifest any divergence indicates that the exchange interaction between magnetite and maghemite magnetic phases may play an important role in this phenomena. Such interaction may imply the presence of unidirectional anisotropy after the FC treatment. To test this suggestion, additional low-temperature experiments are necessary.

The observed divergences prevent the direct application of the low-temperature technique proposed by Moskowitz et al. (1993) to our sediments. Nevertheless interesting downcore changes of low-temperature properties were observed which appear to correlate with changes in redox conditions.

References:

Moskowitz et al., *Earth Planet . Sci. Lett.*, 120, 283-300, 1993.
Tarduno, J.A., and S.Wilkison, *Earth Plan. Sci. Lett.*, 144, 315-326, 1996.
Tarduno, J.A., et al., *Geoph. Res. Lett.*, 25, 3987-3990, 1998.
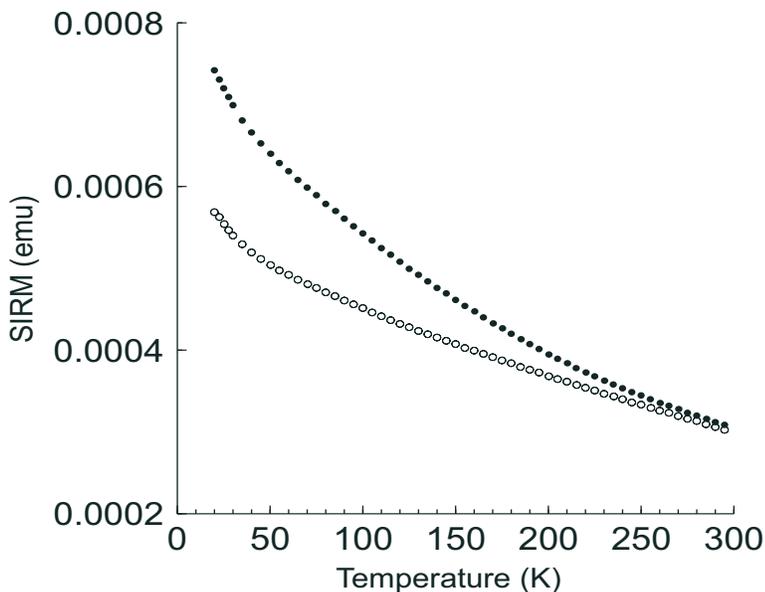
Figure 1. The divergence between zero-field-cooled (open circles) and field-cooled (solid circles) SIRM thermal demagnetization curves observed on pelagic sediments from ODP Site 805C.
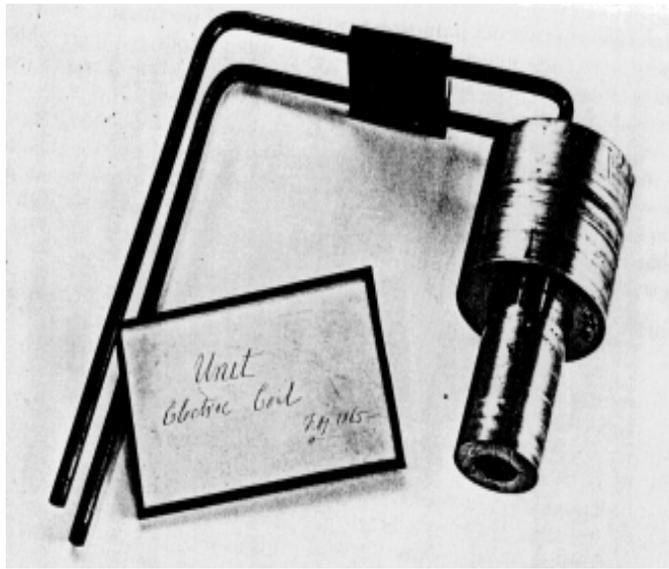
The British Association on Electrical Standards met in Birmingham in 1865 and adopted as a standard of electrical resistance a platinum silver alloy coil, whose resistance was defined as 1 ohmad (later shortened to ohm). Indentical standard coils were distributed internationally; the one shown here was purchased by Faraday for the Royal Institution [Lord Kelvin: His Influence on Electrical Measurements and Units, by Paul Tunbridge, Peter Peregrinus Ltd, 1992.]

Current Abstracts

A list of current research articles dealing with various topics in the physics and chemistry of magnetism is a regular feature of the IRM Quarterly. *Articles published in familiar geology and geophysics journals are included; special emphasis is given to current articles from physics, chemistry, and materials-science journals. Most abstracts are culled from* INSPEC *(© Institution of Electrical Engineers),* Geophysical Abstracts in Press *(© American Geophysical Union), and* The Earth and Planetary Express *(© Elsevier Science Publishers, B.V.), after which they are subjected to Procrustean editing and condensation for this newsletter. An extensive reference list of articles (primarily about rock magnetism, the physics and chemistry of magnetism, and some paleomagnetism) is continually updated at the* IRM. *This list, with more than 4200 references, is available free of charge. Your contributions both to the list and to the Abstracts section of the* IRM Quarterly *are always welcome.*

Alteration, Diagenesis and Remagnetization

Urbat, M., and Dekkers, M. J., 1999, **Peru Basin sediments: diagenetic implications of a low coercivity overprint of the NRM**: *Geophysical Research Letters, v. 26*, no. 5, p. 545-8.
Two populations of magnetite that vary by at least 320 kyr in age coexist in oxic through suboxic Peru Basin sediment. (1) Primary magnetite yields a straightforward magnetostratigraphy (Brunhes Chron-top of Olduvai Subchron). (2) A stable, low-coercivity overprint of the NRM resides in secondary, slightly oxidized SD magnetite that recorded the Brunhes Chron direction. The secondary magnetite appears at the modern Fe-redox boundary and continues downhole to abruptly disappear in the Matuyama Chron. The Verwey transition is apparent in low-temperature remanence measurements (20-300 K) for samples with the overprint.

Domain Theory and Micromagnetic Modeling

Williams, W., and Wright, T. M., 1998, **High-resolution micromagnetic models of fine grains of magnetite**: *Journal of Geophysical Research, v. 103*, no. B12, p. 30537-50.
New high-resolution 3D models of cubic grains of magnetite (0.03μm to 4.0μm) use a resolution of up to 262,144 elements per grain, and confirm the simple flower and vortex states found previously. The classical two-domain (with closure domains) Kittel structure is shown not to be a local energy minimum state for magnetite. The concept of a single-domain to two-domain transition is now seen as a gradual unwinding of a flower state, and PSD grains are shown to be vortex and multiple-vortex states. For grains greater than about 2μm in size, vortices act as nucleation centers for the formation of domain walls. At the largest grain size modeled, the expected features of multidomain grains are seen, with well-defined domain walls, and body domains with their magnetization aligned along the easy axis.

Zhang, K., and Fredkin, D. R., 1999, **Effects of partial surface anisotropy on a fine magnetic particle**: *Journal of Applied Physics, v. 85*, no. 8, p. 6187-9.
Surface effects on fine magnetic particles become very pronounced because of the large surface-to-volume ratio. Using micromagnetic simulations, we have demonstrated that surface anisotropy with the proper sign contributes to the increase of coercivity. Here we model the situation where only part of the particle surface has anisotropy, for an elongate single domain γ-Fe_2O_3 particle. The surface anisotropy energy is added to the total magnetic energy of the particle, and hysteresis loops are obtained by minimizing the total energy at a given applied field. The addition of positive equatorial surface anisotropy enhances the coercivity, but with polar anisotropy the coercivity decreases. In both cases the surface magnetization tends to be tangential to the surface and the magnetiza-

tion reversal is incoherent and starts from the surface.

Magnetic Microscopy and Spectroscopy

Ambatiello, A., Fabian, K., and Hoffmann, V., 1999, **Magnetic domain structure of multidomain magnetite as a function of temperature: observation by Kerr microscopy**: *Physics of the Earth and Planetary Interiors, v. 112*, no. 1-2, p. 55-80.
Room-temperature magneto-optical Kerr effect (MOKE) observations of monocrystalline multidomain magnetites show lamellar domains separated by 180° walls, and closure domains with 71°, and 109°walls on the (110)-plane. Observations on the (111)-plane reveal more complex patterns formed by arrays of closure domains. For high temperature domain observations, a special furnace has been developed which allows domain observations using the MOKE between room temperature and the Curie-point (575°C).

Borchers, J. A., Ijiri, Y., Lind, D. M., Invanov, P. G., Erwin, R. W., Lee, S. H., and Majkrzak, C. F., 1999, **Polarized neutron diffraction studies of exchange-coupled Fe_3O_4/NiO superlattices**: *Journal of Applied Physics, v. 85*, no. 8, p. 5883-5.
In order to understand the interplay between exchange coupling and magnetic structure, we have examined the magnetic ordering of a series of epitaxial Fe_3O_4/NiO superlattices using polarized neutron diffraction techniques. As expected, the net ferrimagnetic moment of the Fe_3O_4 layers aligns parallel to an applied magnetic field. The antiferromagnetic NiO spins order into alternating antiparallel <111> planes as in bulk, but the direction of the spins in the planes is determined by field preparation. The NiO moments tend to align perpendicular to the field. In addition, the relative population of the NiO domains varies as the field is raised. The changes in the antiferromagnetic spin order relative to bulk seem to result from magnetic coupling with the Fe_3O_4 moments.

Kendelewicz, T., Liu, P., Doyle, C. S., Brown, G. E., Jr., Nelson, E. J., and Chambers, S. A., 1999, **X-ray absorption and photoemission study of the adsorption of aqueous Cr(VI) on single crystal hematite and magnetite surfaces**: *Surface Science, v. 424*, no. 2-3, p. 219-31.
The speciation of chromium in overlayers on atomically clean surfaces of single crystal magnetite (Fe_2O_4) and hematite (α-Fe_2O_3) were studied using X-ray absorption spectra collected with synchrotron radiation. Chemically shifted components in the spectra indicate OH- ligands around Cr and Fe. Cr(VI) is reduced to Cr(III) on magnetite (111) surfaces, with rapid reaction kinetics. While Cr adsorbed on the (1102) surface of hematite (Fe_2O_3) remains in the original Cr(VT) form, small amounts are reduced to Cr(III) on (0001) hematite surfaces. This difference is due to the presence of Fe(II) on the (0001) hematite surfaces produced during

Abstracts

3

annealing in a vacuum environment.

Medrano, C., Baruchel, J., and Kvardakov, V. V., 1999, **Unusual magnetization process in haematite investigated by synchrotron radiation diffraction imaging**: *Philosophical Magazine Letters, v. 79*, no. 5, p. 283-8.
The magnetization process of a nearly perfect crystal of haematite is investigated through the observation of domain wall evolution in an applied magnetic field, by white-beam X-ray section topography. The sample is a (111) platelet. The walls are nearly parallel to its main surface. Their contrast changes dramatically with increasing field, but their locations are not altered very much during most of this process, suggesting a magnetization process which occurs mainly by spin rotation within the domains. The very small basal plane anisotropy of haematite and the pinning of the walls by defects results in this unusual magnetization process, which differs from the standard process for ferromagnets.

Paleoclimate and Magnetic Proxy Records

Hounslow, M. W., and Maher, B. A., 1999, **Source of the climate signal recorded by magnetic susceptibility variations in Indian Ocean sediments**: *Journal of Geophysical Research, v. 104*, no. B3, p. 5047-61.
The magnetic susceptibility variations in ODP Hole 722B were previously identified as an outstanding proxy paleoceanographic record, despite diagenetic loss of magnetic minerals. Here we assess the contributions of ferrimagnetic detrital iron oxides, bacterial magnetosomes, and paramagnetic detrital Fe silicate minerals to the magnetic susceptibility signal. In addition to detailed magnetic analyses, mineralogical, morphological, and grain size data have been obtained from representative magnetic extracts. For Hole 722B, (1) magnetic susceptibility is primarily controlled by carbonate dilution; (2) a ferrimagnetic signal, which is restricted to the upper 7 meters below sea floor (mbsf), largely reflects source area aridity; and (3) a paramagnetic susceptibility record below 7 mbsf is coincident in frequency with variations in lithogenic grain size.

Paleomagnetic Field Records and Paleointensity

Cottrell, R. D. and Tarduno, J. A., **Geomagnetic paleointensity derived from single plagioclase crystals**, *Earth and Planetary Science Letters, v. 169*, 1-5, 1999.
We suggest a new approach for the determination of absolute geomagnetic paleointensity that uses single plagioclase crystals to avoid problems caused by alteration during Thellier-Thellier analyses. Transmission electron microscope imaging and rock magnetic data indicate that plagioclase crystals from a recent basalt flow in Hawaii contain pseudo-single to single domain titanomagnetite inclusions. These feldspars yield paleointensity values that agree within error with magnetic observatory data and paleointensity values reported from whole rock samples.

Goguitchaichvili, A. T., Prevot, M., and Camps, P., 1999, **No evidence for strong fields during the R3-N3 Icelandic geomagnetic reversal**: *Earth and Planetary Science Letters, v. 167*, no. 1-2, p. 15-34.
A previous study of the R3-N3 Icelandic reversal, which corresponds probably to the Matuyama-Reunion reversal, provided relatively large virtual dipole moments when the pole is close to equator. To check these former results, obtained using the Shaw paleointensity method, the present authors resampled the very same sections and flows and reanalysed the samples using the Thellier method. An average paleointensity of $11.3\pm3.0\mu T$ during the R3-N3 transition is much less than those previously obtained by the Shaw method.

Kok, Y. S., 1999, **Climatic influence in NRM and [10]Be-derived geomagnetic paleointensity data**: *Earth and Planetary Science Letters, v. 166*, no. 3-4, p. 105-19.
Two independently derived 200-kyr stacked geomagnetic paleointensity records, based on normalized NRM and cosmogenic isotope ([10]Be and ^{14}C) data, show good agreement. Both compilations used mainly the astronomically forced and climatically controlled oxygen isotope stratigraphy to date and synchronize the sedimentary records, while this very curve has several coherent features with the supposedly pure geomagnetic records, suggesting an inadequacy in the normalization technique. Therefore, it is possible that the extraction of the pure paleointensity signal from marine sediments has not always been accomplished.

Kruiver, P. P., Kok, Y. S., Dekkers, M. J., Langereis, C. G., and Laj, C., 1999, **A pseudo-Thellier relative palaeointensity record, and rock magnetic and geochemical parameters in relation to climate during the last 276 kyr in the Azores region**: *Geophysical Journal International, v. 136*, no. 3, p. 757-70.
Pseudo-Thellier relative palaeointensity determinations on a marine core from the Azores, spanning the last 276 kyr, show intensity lows with deviating palaeomagnetic directions at 40-45 ka and at 180-190 ka. The first interval is associated with the Laschamps excursion, while the 180-190 ka low represents the Iceland Basin excursion. Spectral analysis of the rock magnetic parameters and the palaeointensity estimates shows orbitally forced periods, particularly 23 kyr, suggesting that palaeointensity is still slightly contaminated by climate.

Mazaud, A., and Channell, J. E. T., 1999, **The top Olduvai polarity transition at ODP Site 983 (Iceland Basin)**: *Earth and Planetary Science Letters, v. 166*, no. 1-2, p. 1-13.
U-channel data from ODP Site 983 in the vicinity of the top Olduvai polarity transition show a normalized remanence (paleointensity) low with post-reversal recovery in paleointensity but no systematic decay in paleointensity in the Matuyama Chron above the reversal. The virtual geomagnetic pole (VGP) path includes a number of loops over Canada and the North Atlantic, prior to a path over the Americas to a VGP cluster in the South Atlantic, off Argentina. The path then leads to a VGP cluster over India, then a loop over the Caribbean and transits through the

Atlantic to high southerly latitudes. VGP clusters in the transition path are observed at positions which are broadly similar to those seen in the top Jaramillo transition at the same site, may imply a memory effect in the geodynamo spanning successive reversals of the same sense.

Rixiang, Z., Yongxin, P., and Qingsong, L., 1999, **Geomagnetic excursions recorded in Chinese loess in the last 70,000 years**: *Geophysical Research Letters, v. 26*, no. 4, p. 505-8.
Detailed paleomagnetic investigations conducted on the Malan loess (L1) at a well-dated section (Weinan) in the Chinese Loess Plateau revealed two distinct anomalous directional intervals (ADI) accompanied by lower relative paleointensity. Rock magnetic properties and anisotropy of magnetic susceptibility of samples taken from sedimentary horizons carrying the anomalous directions are similar to those taken from outside the ADI. Thus, the anomalous directions are interpreted as geomagnetic excursions. Based on ^{14}C and TL data, the excursions occurred at 27.1-26.0 and 46.8-37.4 kyr BP; the ages are consistent with the ages assigned to the Mono Lake excursion (MLE) and Laschamp excursion (LE), respectively. The result indicates that the MLE and LE were independent geomagnetic excursions. The morphology of LE at this section suggests that the LE might be an aborted geomagnetic reversal.

Schwartz, M., Lund, S. P., and Johnson, T. C., 1998, **Geomagnetic field intensity from 71 to 12 ka as recorded in deep-sea sediments of the Blake Outer Ridge, North Atlantic Ocean**: *Journal of Geophysical Research, v. 103*, no. B12, p. 30407-16.
Paleointensity records obtained by NRM normalization for three cores show consistent short-duration (10^3 years) features regardless of normalizer choice, even though the cores are separated by almost 250 km, suggesting that these are real geomagnetic field signals of at least local extent. A number of differences between our records must be artifacts of sediment remanence acquisition or environmental biases in paleointensity normalization. Major paleointensity features can be correlated with other records from the same extended region. However, differences in the ages and disagreement in magnitude and number of individual features call into doubt the use of these relative paleointensity records for high-resolution chronostratigraphic correlation on a broader scale or for estimating absolute paleointensity.

Shaw, J., Yang, S., Rolph, T. C., and Sun, F. Y., 1999, **A comparison of archaeointensity results from Chinese ceramics using microwave and conventional Thellier's and Shaw's methods**: *Geophysical Journal International, v. 136*, no. 3, p. 714-18.
Microwave excitation of magnetic grains can create a TRM without significantly heating the bulk samples, thereby avoiding thermal alteration. We apply this microwave technique to a collection of Chinese ceramics covering the time interval 2700-7500 yr BP, previously studied using both Thellier's and Shaw's palaeointensity methods. Although an acceptable agreement was found between those two methods, the equivalent virtual

axial dipole moments (VADMs) were significantly lower than for the global model of McElhinny and Senanayake (1982). The microwave technique has provided VADMs much closer to the global model.

Tanaka, H., 1999, **Theoretical background of ARM correction in the Shaw palaeointensity method**: *Geophysical Journal International, v. 137*, no. 1, p. 261-5.
A computer simulation using Jaep's ARM model (based on Néel's relaxation theory) was made for an ensemble of single-domain grains of magnetite with a log-normal grain distribution. Variations in the capacities of ARM and TRM were calculated when volume or coercivity was changed up to ±50 per cent. If the grain interaction effect is ignored in ARM, the change in ARM capacity due to a change in volume is almost identical to that of TRM. For a more realistic case with grain interaction effects in ARM, the change in capacity due to a change in volume is different in ARM and TRM, although the difference is about 6-7 per cent at most for a change of ±20 per cent in ARM capacity. It is suggested that ARM correction should be limited to those results in which the ratio of ARM_1/ARM_2 is moderately close to unity.

Remanence and Magnetization Processes

Bottoni, G., Candolfo, D., Cecchetti, A., and Masoli, F., 1999, **Analysis of the magnetization switching using the rotational hysteresis integral**: *Journal of Magnetism and Magnetic Materials, v. 193*, no. 1-3, p. 329-31.
The relation of the rotational hysteresis integral with the magnetization switching mode is experimentally analysed in materials which are subjected to different treatments which can modify the magnetization switching mode. As expected, the value of the integral depends on the basic processes of magnetization. They evolve with the evolution of the switching in the expected way, both when the switching changes from wall motion to rotation of the magnetization, and when, in single-domain particles, the rotation occurs with different reversal modes.

Dunlop, D. J., 1998, **Thermoremanent magnetization of nonuniformly magnetized grains**: *Journal of Geophysical Research, v. 103*, no. B12, p. 30561-74.
SD TRM is a frozen high-temperature partition between two microstates: spins parallel or antiparallel to an applied magnetic field. Nonuniformly magnetized grains have a much greater choice of microstates (local energy minimum or LEM states), and partitioning among various LEM states continues to change during cooling. Because of the lower remanence capacity of nonuniform microstates compared to the uniform SD state, TRM intensity decreases as grain size increases. Thermal demagnetization of TRM begins just above room temperature and continues to the Curie point, quite unlike the sharp "unblocking" of SD TRM. This continuous demagnetization, resulting from changes in microstates driven by the changing internal demagnetizing field during heating, profoundly affects the separation of different

components of natural remanent magnetization and the determination of paleomagnetic field intensity.

Halgedahl, S. L., 1998, **Barkhausen jumps in large versus small platelets of natural hematite**: *Journal of Geophysical Research, v. 103*, no. B12, p. 30575-89.
To better understand the physical links among hysteresis properties, defect distributions, and grain size, Barkhausen jumps have been studied in individual platelets of natural hematite during hysteresis. Both Bitter patterns and hysteresis curves have been investigated in two very different groups of platelets: large, 1-mm-sized platelets with coercive forces (Hc) in the range of 2-5 mT, and much smaller, 100μm-sized platelets, with Hc in the 10-14 mT range. Single platelets were cycled through both major and minor hysteresis, in order to determine (1) the changes of magnetic moment caused by Barkhausen jumps and (2) how these changes may depend on grain size and the critical field H_{crit} required to unpin a wall from a defect.

Prozorov, R., Yeshurun, Y., Prozorov, T., and Gedanken, A., 1999, **Magnetic irreversibility and relaxation in assembly of ferromagnetic nanoparticles**: *Physical Review B, v. 59*, no. 10, p. 6956-65.
Measurements of the time-logarithmic decay of the magnetization are described for three Fe_2O_3 samples composed of regular amorphous, acicular amorphous, and crystalline nanoparticles. A new model in which the barrier for magnetic relaxation depends on the instantaneous magnetization (and therefore on time) yields a natural explanation for the time-logarithmic decay of the magnetization. Interactions between particles as well as shape and crystalline magnetic anisotropies define an energy scale that controls the magnetic irreversibility.

Zitzelsberger, A., and Schmidbauer, E., 1999, **Temperature dependence of magnetic hysteresis properties, and thermoremanent and anhysteretic remanent magnetization of stress-controlled synthetic 1-125μm titanomagnetite ($Fe_{2.3}Ti_{0.7}O_4$) particles**: *Geophysical Journal International, v. 136*, no. 3, p. 505-18.
Hysteresis properties were measured as a function of grain size for milled and afterwards annealed or etched synthetic 1-125μm $Fe_{2.3}Ti_{0.7}O_4$ (TM70) spinel particles. In general, there is a notable alteration of magnetic parameters by annealing or etching that marks a change of internal stresses caused by dislocations. From the results of remanent coercive force Hcr versus grain size D for annealed particles, Hcr varies as D^{-m}, m≈0.60, in the whole size range. For annealed particles, the total weak-field (160 A m^{-1}) TRM has a constant value for 1≤D≤6μm, and obeys a power-law (TRM ∝ D^{-P}, P≈0.53) in the range 6≤D≤40-50μm; for larger particles a smooth transition takes place to a constant value typical for MD particles.

Synthesis and Properties of Magnetic Minerals

Abe, M., Ishihara, T., and Kitamoto, Y., 1999, **Magnetite film growth at 30°C on organic

monomolecular layer, mimicking bacterial magnetosome synthesis**: *Journal of Applied Physics, v. 85*, no. 8, p. 5705-7.
At 30°C magnetite (Fe_3O_4) films were grown, 5μm in thickness, by flowing a mixed gas of $O_2/N_2=1/2000$ on lipid monomolecular layers of arachic acid spread on an aqueous solution of $FeCl_2$. The ordered array of the OH groups of the lipid layer stimulated the nucleation and growth of the Fe_3O_4 films, similar to bacterial magnetosome (Fe_3O_4 crystals) synthesis in which the OH groups on the cytoplasmic membrane stimulate the surface growth of Fe_3O_4.

Hibma, T., Voogt, F. C., Niesen, L., van der Heijden, P. A. A., de Jonge, W. J. M., Donkers, J. J. T. M., and van der Zaag, P. J., 1999, **Anti-phase domains and magnetism in epitaxial magnetite layers**: *Journal of Applied Physics, v. 85*, no. 8, p. 5291-3.
Anti-phase boundaries (APBs) cause anomalous magnetic behavior in epitaxial thin films of magnetite. Transmission electron microscopy images confirm that APBs are present in our Fe_3O_4 films grown by molecular beam epitaxy on MgO(100). To explain the deviating saturation and the superparamagnetic behavior of thin Fe_3O_4 films at the same time, the magnetic coupling over the APB must be dramatically reduced due to spin disorder along the boundaries.

Lee, H. S., Lee, W. C., and Furubayashi, T., 1999, **A comparison of coprecipitation with microemulsion methods in the preparation of magnetite**: *Journal of Applied Physics, v. 85*, no. 8, p. 5231-3.
Coprecipitation and microemulsion were used to prepare nanosized magnetite (average particle sizes of samples A and B were 8.16 and 2.24 nm, respectively). The saturation magnetization of sample A at 300 K was 57.2 emu/g, but sample B was not saturated even 7.0 T. The blocking temperature for sample B was 17 K and the crystalline anisotropy energy was $1.2*10^5$ J/m^3. At 5 K, sample B is ferrimagnetic with σ_s=7.62 emu/g. This value is much lower than the σ_s=65.4 emu/g of the crystallized sample A at 50 K. Mössbauer spectra showed that sample A was ferrimagnetic at room temperature, but sample B was superparamagnetic at T>Tb (critical blocking temperature).

Rudee, M. L., Smith, D. J., and Margulies, D. T., 1999, **Evidence for charge ordering at room temperature in Fe_3O_4**: *Physical Review B, v. 59*, no. 18, p. R11633-6.
We report observations at room temperature and above of a new form of charge ordering in thin films of magnetite. This phenomenon of charge ordering on tetrahedral sites is unrelated to the well-known low-temperature ordering on octahedral sites that occurs below 120 K. The charge ordering is visible in electron micrographs, which clearly show disorganized boundaries between regions of regularly arranged charge ordering. Ordering of this type in magnetite may not have been observed previously because of insufficient purity and perfection of the materials studied. However, we suspect that similar charge ordering is likely in other metal oxides of high crystal quality where metal ions have mixed-valence states.

Sichu, L., John, V. T., Rachakonda, S. H., Irvin, G. C., McPherson, G. L., and O'Connor, C. J., 1999, **Higher crystallinity superparamagnetic ferrites: Controlled synthesis in lecithin gels and magnetic properties**: *Journal of Applied Physics, v. 85*, no. 8, p. 5178-80.
We have synthesized γ-Fe_2O_3 nanoparticles in a novel organohydrogel medium. Transmission electron microscopy observations indicate that the particles are spherical and range in size from 15 to 25 nm. The particles exhibit superparamagnetic behavior with a blocking temperature of 24 K and a coercivity of 1600 G at 2 K. Both the blocking temperature and the coercivity of ferrites synthesized in the lecithin gel were higher than those synthesized in water-in-oil microemulsions. The sizes of the domains are the same for these two kinds of particles, while the crystallinity may be higher for the particles synthesized in the lecithin gel media.

Sorescu, M., Brand, R. A., Mihaila-Tarabasanu, D., and Diamandescu, L., 1999, **The crucial role of particle morphology in the magnetic properties of haematite**: *Journal of Applied Physics, v. 85*, no. 8, p. 5546-8.
Haematite particles of four different morphologies (polyhedral, platelike, needlelike and disk shaped) and sizes (1.4, 7.4, 0.2, and 0.12μm, respectively) were synthesized by the hydrothermal method, characterized by transmission electron microscopy combined with electron diffraction, and studied by transmission Mössbauer spectroscopy in the temperature range 4.2-300 K. In all cases, a weak ferromagnetic (WF) phase was present above the Morin temperature of 230 K and found to coexist with an antiferromagnetic (AF) phase below this temperature. However, the populations of the two phases at 230 K were demonstrated to depend on the morphology of the particles. Moreover, the WF and AF phases exhibit a different dependence of the magnetic texture on temperature and particle morphology.

Soszka, W., Kim-Ngan, N. T. H., Sitko, D., Jaglo, G., and Kozlowski, A., 1999, **Ion scattering from the single-crystal magnetite Fe_3O_4 under the Verwey transition**: *Vacuum, v. 54*, no. 1-4, p. 83-7.
Energy spectra of ions scattered from a cleaved surface of a single-crystal Fe_3O_4 at small scattering angles show the Verwey transition around 120 K, corresponding to the transition from dynamic disorder to long-range order in the distribution of Fe^{2+} and Fe^{3+} ions in octahedral sites. This transition is accompanied by a structural transition from cubic FCC to a monoclinic structure. The observed change in the ion scattering under this transition is due to the increase of the neutralization probability and the change of the target material transparency.

Other

Ibragimov, S. Z., Yasonov, P. G., and Denisov, I. G., 1998, **A component expansion of the temperature-dependent saturation magnetization of a ferrimagnetic fraction of rocks**: *Izvestiya, Physics of the Solid Earth, v. 34*, no. 12, p. 1041-4.
A method proposed for the expansion into components of the temperature-dependent saturation magnetization I_s (T) of rock samples containing several ferrimagnetic phases is based on the assumption of the additive summation of the phase saturation magnetizations. The technique was tested on samples with known ferrimagnetic composition, and can be applied to quantitative analysis of a multiphase rock fraction.

...Units
continued from page 1

A Funny Thing Happened
on the Way to SI

In fact, several interesting things happened, in addition to the straightforward transition from centimeters and grams to meters and kilograms.

In the cgs system of units that evolved out of Gauss's measurements, three of the basic magnetic quantities have exactly the same dimensions: *H*, *B*, and *M* (volume-normalized magnetization; $M=m/V$). The *meanings* of these quantities, however are not identical, and they are specified with different unit names, respectively Oersted, Gauss, and emu/cm³. The relationship that ties them together is:

$$B=H+4\pi M$$

In vacuo, where *M* is zero, *B* and *H* are dimensionally and numerically equal under the cgs system, and they are often treated interchangeably.

In the newer SI (Système internationale d'unités) formulation,

$$B=\mu_0(H+M)$$

Two differences are apparent: the factor 4π has disappeared, and a new factor μ_0 has been added.

Let's begin with the 4π. One of the significant changes introduced in SI is *rationalization*, which means, in effect, that quantities are defined in such a way that factors involving π do not appear in Maxwell's equations. By a sort of conservation principle, the removal of π from some equations results in its reappearance in others. For example, if a radial vector field (such as the electric field at unit distance from a unit charge) is defined to have unit intensity, then the associated total flux (integrated surface-normal field component) must have a magnitude of 4π. Maxwell's equations are formulated not directly in terms of vector fields, but in terms of their divergences (or surface flux integrals) and curls (or circuit line integrals), and removal of the respective factors of 4π and 2π from these requires the appearance of reciprocal factors in the direct field equations. In devising a coherent system of definitions and units, one is free to choose between these two arrangements, and long before the eventual adoption of SI, rationalization was an issue. Oliver Heaviside wrote, ca 1890: "the unnatural suppression of 4π in the formulas of central force, where it has a right to be, drives it into the blood, there to multiply itself, and afterward break out all over the body of EM theory." (The Heaviside-Lorentz system is a rationalized Gaussian cgs system that never attained wide usage.)

Much Ado About Nothing

The factor μ_0 known as the permeability of free space, represents a more fundamental departure of SI from the cgs system. The notion that free space has a magnetic permeability, residing not in matter but in the nothingness of space itself, has somewhat ethereal overtones. There is an implicit μ_0 in cgs, where it is a dimensionless constant equal to unity. In the SI system μ_0 differs not only in numerical value, but also in physical dimensions. Thus *B* in the SI system has different units, and a different dimensionality than *H* and *M* (and thus I felt compelled to rewrite the description of Gauss' experiment above). Much of the difficulty in coping with the arduous cgs-SI transition [Payne, 1986; Shive, 1986; *IRM Quarterly* v. 4 n. 1] has arisen because dimensional analysis, a standard tool for unit conversion, fails here.

The simplicity of form of μ_0 in cgs has historical roots. Before Oersted's discovery, electricity and magnetism were considered separate phenomena, and quantification schemes evolved independently, each internally self-consistent and self-contained. Coulomb demonstrated that the force between electric charges or magnetic poles obeyed an inverse square law, the force in each case being proportional to the product of charges (or poles) and to the reciprocal square of their separation:

$$F = C_e q_1 q_2/r^2$$

The product $C_e q_1 q_2$ therefore must have the same dimensions as Fr^2. Lacking additional constraints, one is free to define the electrostatic proportionality constant C_e as dimensionless and equal to unity, thereby specifying the dimensions and units of *q* (1 statcoulomb = 1 $cm^{3/2}g^{1/2}s^{-1/2}$). The electrostatic system of units (esu) originated in this way, as did the parallel emu system for magnetostatic quantities.

The discovery of electromagnetism, however, placed additional constraints on the electric and magnetic proportionality

THE MAGNETIC Chef

Christoph Geiss
*http://
www.geo.umn.edu/orgs/
irm/people/cgeiss/
index.htm*

Bon Appetit Cafe
rating: ***

Today I reveal the secret of graduate student recruiting at the IRM. Some of you might think that Brian Carter, our latest grad student, came here because of our well equipped lab, Subir's fame, Bruce's bugs or Mike's unbeatable charm. Wrong, dead wrong! Brian picked the IRM over all these other top-notch research institutions because we took him to the Bon Appetit Café. The Bon Appetit Café (421 14th Ave. S.E.) started out as a simple juice bar, probably selling a large variety of vegetable and fruit juices and healthy sandwiches (that was before we took Brian there). Well, healthy juice bars don't do too well around here, so they added beer (still juice as many of you might argue) and, later on, greasy fries, burgers and a bunch of pool tables in the back room. Today, the big sign outlining the benefits of fruit and vitamins is still there, but Bon Appetit Café is more or less the only place on campus where you can get beer and shoot pool without having to watch seven different kinds of boring American sports and commercials on 25 screens. The beer is cheap, running from 6.50/pitcher (domestic) to 12.00/pitcher (Guinness). A pitcher of Summit Pale Ale, which is good local stuff (brewed in St Paul, but it does not qualify as "domestic"), costs 10.50. Pool is cheap too (75 cents/game) if you don't mind that half the pool tables are in bad shape and the cues are even worse (good excuse for poor plays!). The guys bathroom is covered in blood red gang graffiti and if you want to really fit in bring a pair of army pants and boots and pierce your nose/tongue/eyebrows. Curious? Check out their web-site at www.bon-appetit-cafe.com, but don't be too surprised. At lunchtime the crowd is quite different: Last week we saw two old grey-haired ladies munching their burgers, some students did their homework and one guy even wore a tie. The service is friendly, minimal and fast. Sandwiches are surprisingly good and different from the Subway-Blimpie whatsoever fare. You can get all the ordinary stuff such as chicken club, 97.5% fat free ham, etc., but also some more interesting stuff like an Avocado sub or a filled grape-leave sandwich. Prices range around 5 bucks for a decent sandwich, fruit juices are around 2 bucks for a 12oz mug. They do have softdrinks, but who orders a Pepsi in a juice bar? Don't bother with the fruit cocktails, they are mostly ice. The (hopefully) real juices are the same price, and don't unwrap that grape-leave sandwich - otherwise you have the grape leaves rolling on the floor. The Bon Appetit is a great place for a beer on Friday night and a decent sandwich all week long.

...Units

constants. Ampere's law quantifies the force per unit length, *f*, between parallel filamentary currents *i*:

$$f = 2C_m i_1 i_2/r$$

where $C_m = \mu_0/4\pi$ is the same as the magnetostatic proportionality constant. Since $i=dq/dt$, it is easy to show that the ratio C_e/C_m must have dimensions of L^2/T^2, i.e., a velocity squared (in fact it is none other than the square of the speed of light c^2). Both C_e and C_m *cannot* therefore be dimensionless *in a coherent system*. The emu and esu sytems thus required separate units *for everything else*, differing by factors of *c* or c^2; for example an abcoulomb (the emu unit of electric charge) equals $3x10^{10}$ statcoulombs (the conversion factor equaling *c* in cm/s). This was a remarkably cumbersome arrangement (although, on the plus side, it allowed the electric and displacement fields to have exactly the same units as B and H). To make matters worse, a third set of units for electrical and magnetic quantities emerged, known as "practical" units. These are the familiar ampere, volt, coulomb, etc., and their practicality derived primarily from numerical magnitude convenience.

In 1901, Giovanni Giorgi proposed, at a meeting of the Italian Electrical Engineering Society, that the "practical" units could form the basis of a fully coherent system of absolute units of measure for electromagnetism and mechanics, if combined with the meter, kilogram and second, together with one additional fundamental unit, to be selected from the basic units of electricity and magnetism. In 1935 the International Electrotechnical Commission met in Brussels and adopted the MKS system, leaving open the choice of a fourth fundemental unit. Although the ohm was favored by many as an easily measurable and manufacturable material standard, the ampere ultimately prevailed in the MKSA system, which formed the essential basis of the SI, adopted in 1960 by the General Conference of Weights and Measures.

As You Like It

A system of units is like a piece of music: each "works" according to its own internal consistency or logic. Often a piece of music is transposed from one key to another, to make it more playable on a particular instrument or group of instruments. Transposition maintains the internal logic of the piece, rescaling frequencies but preserving the musical structure and ideas. Similarly, transformation of physical units from one system to another must preserve the melody and harmony of the laws of electromagnetism, while making them more widely playable. The guttural mating call of the emu, in any other key, would sound as sweet.

Bibliography

Burtt, E. A., 1954, **The Metaphysical Foundations of Modern Science**, Garden City NY, Anchor, 352 p.

Units

Thompson, William (Lord Kelvin)

*b. June 26, 1824, Belfast;
d. Dec. 17, 1907, Largs*

Kelvin derived the absolute thermometric scale that bears his name, based on the thermodynamic work of Carnot and others. Kelvin himself played an important role in formulating the laws of thermodynamics. He is best remembered in the geosciences for calculating an uncomfortably small age of 100 Ma for the earth, based on conductive heat loss with no internal heat sources. The Kelvin mariner's compass (shown) improved on earlier designs in compensating for both the magnetism and the motion of ships. Kelvin was a key figure in the establishment of international units and standards for electrical and magnetic measurements.

RAC Rotation

Dennis Kent (LDEO and Rutgers University) has stepped down from the *IRM*'s Review and Advisory Committee (*RAC*) after five effective and helpful years of service. The *RAC* evaluates all of the Visiting Fellowship proposals we receive and provides strategic guidance in annual meetings at *IRM*, and approximately every two years the *RAC* undergoes a partial membership exchange. Dennis' insight and frank input have been very important to our success as a shared resource for the international paleomagnetic and rock magnetic research community.

As we thank Dennis for his guidance, we also welcome two new members, **Lisa Tauxe** (Scripps / University of California - San Diego) and **Jim Channell** (University of Florida - Gainesville), who will help to maintain the *RAC*'s high level of expertise in paleomagnetism and applied rock magnetism. They will join **Dan Dahlberg** (Physics Dept., University of Minnesota), **Sue Halgedahl** (University of Utah), **Friedrich Heller** (ETH-Zurich), **Ken Kodama** (Lehigh University), and chair **John King** (University of Rhode Island) on the reconstituted *RAC*.

Two New Doctorates

Former *IRM* graduate students **Stefanie Brachfeld** and **Christoph Geiss** have undergone the metamorphosis to *IRM* post-docs, after recently completing their dissertations. Stefanie's work on "Separation of Geomagnetic Paleointensity and Paleoclimate Signals in Sediments: Examples from North America and Antarctica" develops methods to recognize and remove normalization artifacts resulting from magnetic grain-size variations, documents a prime paleofield record in Lake Pepin (Minnesota) and investigates the climatic forcing mechanisms behind cyclic and non-cyclic susceptibility variations off the Antarctic Peninsula. Christoph's work on "The Development of Rock-Magnetic Proxies for Paleoclimate Reconstruction," establishes protocols for integration of magnetic and nonmagnetic data acquisition and analysis, and applies them to sediments from Pittsburg Basin (Illinois) and Kirchner Marsh (Minnesota). Look for their "Postdoctoral Transitions" article in a future issue for more details on their continuing research.

Collector's Series #12

from *The Life of Lord Kelvin*, by Sylvanus P. Thompson, 1976 (second edition), Chelsea Publishing

KELVIN

Garland, G. D., 1979, **The contributions of Carl Friedrich Gauss to geomagnetism**, *Historia Mathematica, v. 6*, p. 5-29.

Glazebrook, R. T., Abraham, H., Page, L., Campbell, G. A., Curtis, H. L., and Kennelly, A. E., 1933, **Systems of Electrical and Magnetic Units: Papers Presented before the American Section, International Union of Pure and Applied Physics, Chicago, June 24, 1933**: *Bulletin of the National Research Council, v. 93*, p. 1-112.

Jauncey, G. E. M., and Langsdorf, A. S., 1940, **M.K.S. Units and Dimensions and a Proposed M.K.O.S. System**: New York, MacMillan, 62 p.

Meyer, H. W., 1971, **A History of Electricity and Magnetism**: Cambridge, MA, MIT Press, 325 p.

Payne, M. A., 1981, **SI and gaussian cgs units, conversions and equations for use in geomagnetism (also see errata)**: *Physics of the Earth and Planetary Interiors, v. 26*, p. P10–P16.

Shive, P. N., 1986, **Suggestions for the use of SI units in magnetism**: *Eos, Transactions of the American Geophysical Union, v. 67*, p. 25.

Thomson, W., 1872, **Reprint of Papers on Electrostatics and Magnetism**: London, MacMillan, 592 p.

Tunbridge, P., 1992, **Lord Kelvin: His Influence on Electrical Measurements and Units**, IEE History of Technology Series: London, Peter Peregrinus, 107 p.

Yavetz, I., 1995, **From Obscurity to Enigma: The Work of Oliver Heaviside, 1872-1889**, Basel, Birkhauser, 334 p.

I R M
Institute for Rock Magnetism